JOURNAL OF AIRCRAFT
Vol. 36, No. 4, July–August 1999

Decision Theoretical Approach to Pilot Simulation

Kai Virtanen,* Tuomas Raivio,† and Raimo P. Hämäläinen‡
Helsinki University of Technology, FIN-02015-HUT, Espoo, Finland

We simulate and analyze pilot decision making in one-on-one air combat by using an influence diagram. Unlike most of the existing approaches, an influence diagram graphically describes the factors of a decision process and explicitly handles the decision maker's preferences under conditions of uncertainty. In the pilot decision model, the possible combat situations related to each maneuver alternative are associated with a probability and a utility. Influence diagram analysis produces a probability distribution of the overall utility that represents the successfulness of a maneuver and gives information to make rational maneuvering decisions. Sensitivity analysis determines the impacts of different factors on the outcome of the maneuvering decision. The effects of sensor information that will reduce the uncertainty of the model are evaluated with Bayesian reasoning. The model can be utilized in the analysis of a single decision situation or as an automated decision-making system that selects combat maneuvers in air combat simulators.

I. Introduction

ANALYSES of air combat tactics and technologies as well as pilot training are expensive tasks, and not all air combat situations can be analyzed in practice. Optimization, game theory, and simulation are widely used methods in analyzing combat tactics and technologies. Optimal trajectories for a single aircraft can be derived by optimal control theory.[1,2] Certain parts of air combat can be described as pursuit–evasion games,[3] but if the roles of the players are not known a priori, simulation remains as the only practical approach to model and analyze air combat. Thus different batch and real-time-piloted air combat simulators have been developed.[4–7] Batch simulators allow the study of combat tactics and aircraft performance in a controlled and repeatable environment. Real-time-piloted simulators enable tactical experimentation and training of human pilots in a realistic environment. Simulators of both type utilize computer-guided aircraft.

One of the main components of a computer-guided aircraft is a model that imitates pilot decision making. A decision model represents decision situations of a pilot for which the outcome of any particular action is at least partially uncertain and the available information is incomplete. A model must be able to analyze the irregular flow of incoming data that describes a dynamically evolving environment. Furthermore, a decision situation usually involves competing objectives, such as the need to achieve a firing position and simultaneously to avoid the opponent's weapons.

In this paper a new tool from decision analysis (see Refs. 8–11), the influence diagram,[12] is applied to model the decision problems of a pilot during one-versus-one air combat. The pilot decision model offers a tool for analyzing different combat situations and produces reasonable combat decisions that can be used in simulation. Although influence diagrams have already been applied to mission planning,[13] pilot decision making has not been modeled with this tool.

In the pilot decision model, competing objectives are measured in terms of attributes, like the distance to the opponent, and velocity. The state of air combat defines the attribute values that are mapped onto a commensurable utility scale by use of single-attribute utility functions.[10] Finally, the single utilities are aggregated to evaluate the different states of air combat. On the other hand, the model associates probabilities with states, and the results of influence diagram analysis give probability distributions of utility for each decision alternative. The decision is based on a selected decision criterion. For example, if the decision maker is prepared to accept the utility theoretical definition of rationality (see Ref. 11), the alternative that provides the highest expected utility (EU) is chosen. The important and critical factors of the given combat situation are identified by sensitivity analysis. Value and effects of information-gathering activities are analyzed with Bayesian reasoning (see, e.g., Ref. 9).

In this paper, the terms *decision maker* and *pilot* refer to a human expert whose opinions and preferences are to be captured into the decision model. The players of one-on-one combat are called *the simulated decision maker* and *the opponent.*

This paper is organized as follows. First, currently existing approaches for simulating pilot decision making are shortly surveyed. In Sec. III, a short introduction to influence diagrams is given. The pilot decision model based on an influence diagram is described in Sec. IV. The use of the model is demonstrated through example decision situations in Sec. V. In Sec. VI, improvements for refining the structure of the model are suggested and the utilization of the model in simulation is proposed. Furthermore, ideas related to the extension of the approach to M-on-N engagement are given. Finally, concluding remarks appear in Sec. VII.

II. Related Approaches

In the existing air combat simulators, decision-making models are knowledge-based expert systems,[5,7,14] or heuristic-value-driven systems.[6] In addition, discrete game approaches are proposed.[15,16] In these systems, decisions are made at discrete time instants. The possible states of a combat after a given planning horizon are first determined by projecting each maneuver alternative into the future and by predicting the state of the opponent. Then a score is associated with each predicted combat state. Finally, the maneuver alternative that leads to the highest score is executed.

In the simplest rule-based systems, states are evaluated by predetermined combat geometry rules.[17] More advanced systems[5] utilize a fixed set of questions representing different goals. A system associates a single value between zero and one to each goal, depending on the degree to which the state attains a goal. The total value of each maneuver alternative is obtained by calculating the weighted sum of the goal specific values. The weights characterize the relative importance of the goals. States can also be scored by an explicit function that maps the combat situation onto a value scale.[6]

A somewhat different approach is taken in Ref. 15, in which game theoretical analysis is adopted in one-on-one air combat. The consequences of possible maneuvers are evaluated with a nonlinear

Presented as Paper 98-4537 at the AIAA Modeling and Simulation Technologies Conference, Boston, MA, 10–12 August 1998; received 13 October 1998; revision received 31 March 1999; accepted for publication 2 April 1999.

*Researcher, Systems Analysis Laboratory, P.O. Box 1100; kai.virtanen@hut.fi. Member AIAA.

†Assistant Professor, Systems Analysis Laboratory, P.O. Box 1100; tuomas.raivio@hut.fi.

‡Professor, Director of the Systems Analysis Laboratory, P.O. Box 1100; raimo@hut.fi.

scoring function. One player tries to maximize the score and the other tries to minimize it. Then the maneuver is determined by a zero sum matrix game (see, e.g., Ref. 18). The scoring function is versatile but it does not take uncertainty into account. Ref. 16 presents an extended game in which the score is assumed to be probabilistic and the maneuvering decision is made by solving a game tree. The tree is pruned by choosing the decision alternative, with the highest score for one player and the decision alternative with the lowest score for the other player.

Decision theoretical models and knowledge-based expert systems are designed to model and improve human decision making. However, the approaches are based on quite different principles. Decision analytical models apply utility theory and the axioms of probability.[10] Expert systems follow logical and computational techniques. These systems typically have problems in dealing with decision making under uncertainty, since expert systems developers seldom pay attention to the modeling of human preferences and attitudes toward risk.[19] A realistic model for decision making under uncertainty should take into account the decision maker's preferences explicitly.

In an influence diagram model, utility functions describe the preferences. Tradeoffs between competing objectives are characterized by the weight parameters in the utility function, whereas in rule-based systems the tradeoffs must be expressed explicitly. Furthermore, a diagram can be constructed, validated, and updated together with pilots because it is easily understood by individuals who have only little decision theoretical background. In rule-based systems, pilots can validate and analyze models only by analyzing simulation results. Further differences are discussed in Ref. 19.

III. Influence Diagram

An influence diagram[12] is a directed acyclic graph that graphically represents a decision process. For more technical details, see Ref. 20. A diagram consists of decision, chance, and deterministic nodes and arcs connecting them. A decision node contains different decision alternatives and can have numerical values associated with each alternative. A chance node represents an uncertain event or a continuous or discrete random variable and has a numerical value and probability associated with each outcome. Deterministic quantities or variables are modeled by deterministic nodes whose value is either a constant or a function of its inputs. In the graphical representation of influence diagrams, decision nodes are usually squares, probabilistic-node ovals and deterministic-node squares with rounded corners.

Arcs in a diagram show how the elements interact with each other. The meaning of the arcs depends on their destination node. Conditional arcs leading into a chance or deterministic node represent probabilistic or functional dependence. They do not necessarily imply causality, although they often do. Informational arcs pointing to a decision node imply time precedence. They show which quantities are known to a decision maker before an action is taken.

Each diagram contains one deterministic utility node that has no successors. It includes a utility function that models the decision maker's preferences and, in practice, evaluates the possible consequences of the decisions. Consequences are described by a set of continuous or discrete attributes that are related to the objectives. A single-attribute utility function maps an attribute onto a utility that is a commensurable measure for the goodness of attributes. Finally, the single-attribute utilities are combined by an aggregating function.

In the decision science literature, the two common aggregating functions are additive and multiplicative. The additive utility function is a linear combination of single utilities:

$$u(x_1, \ldots, x_n) = \sum_{i=1}^{n} w_i u_i(x_i) \tag{1}$$

where x_i is the attribute i, u_i is a single-attribute utility function, and w_i are positive weights that represent the importance of the attributes and sum up to 1. The additive model is appropriate when the attributes are mutually utility independent (see Ref. 10). Otherwise, a multiplicative form can be used. It is composed by adding product terms of single utilities to Eq. (1). In practice, the utility functions are extracted from the decision maker using appropriate methods (see, e.g., Refs. 10 and 21).

In an influence diagram, probability distributions can be updated by Bayesian reasoning in which the subjective probability interpretation[22] is utilized. A subjective probability $P(\theta)$ represents the decision maker's degree of belief in the occurrence of an event θ based on the decision maker's current information. A decision maker can exploit several methods for assessing subjective probabilities (see, e.g., Ref. 23).

Let us assume that only a finite number of outcomes of the uncertain event are possible and label these outcomes $\theta_1, \ldots, \theta_n$. The decision maker's beliefs on the different outcomes are given by the subjective prior probabilities $P(\theta_1), \ldots, P(\theta_n)$ such that

$$\sum_{i=1}^{n} P(\theta_i) = 1$$

These beliefs will be utilized if a decision must be made immediately. However, before the decision instant, the decision maker observes that an event D has occurred. The decision maker now will decide based on his or her posterior probabilities $P(\theta_1 \mid D), \ldots, P(\theta_n \mid D)$ which can be formed by using Bayes' theorem

$$P(\theta_k \mid D) = \frac{P(D \mid \theta_k) P(\theta_k)}{\sum_{j=1}^{n} P(D \mid \theta_j) P(\theta_j)} \tag{2}$$

Here $k = 1, \ldots, n$, and the terms $P(D \mid \theta_k)$ are called the likelihood probabilities. They mean the probability that the event D occurs under the supposition that the outcome of the uncertain event is θ_k.

In addition to discrete outcomes, continuous outcomes can be used as well. Then, the outcome of an uncertain event belongs to an interval of real numbers. The decision maker's belief on the outcome and the likelihood probability are given by continuous probability distributions and the summation in Eq. (2) is replaced with integration.

A complete influence diagram associates a probability and a utility with each possible consequence of the decision. An influence diagram analysis determines probability distributions of utility associated with each decision alternative. The best decision alternative can be chosen on the basis of these distributions. The decision criterion might be, for example, maximum expected utility. It should be noted, however, that expected utilities are not perfect indicators of what might happen, as the risk of the alternatives varies. Thus the decision alternative with the highest expected utility can also lead to a worse outcome with a certain positive probability.

A. Connection with Decision Trees

Decision trees (see, e.g., Ref. 8) are also a graphical representation of decisions, uncertainties, and values. They are closely linked to influence diagrams, as any diagram can be converted into a symmetric decision tree, although this procedure may require the application of Bayes' theorem. As in influence diagrams, square nodes represent decisions and oval nodes chance events. Branches coming from a decision node correspond to decision alternatives and branches from a chance node represent the possible outcomes of a chance event. A path through the tree, from the root to a leave node, is a combination of specific decision alternatives and chance outcomes. The path represents the possible consequence of the corresponding decision, and the utility of this consequence is specified at the end of the path.

Decision trees and influence diagrams have different advantages in modeling decisions. Diagrams provide compact representation of decision problems by hiding many details of less interest, whereas complex problems may lead to large trees. Thus influence diagrams are ideal for obtaining overviews of decision problems and communicating with an expert of the application area. However, both approaches are useful and complement each other.

B. Numerical Solution Techniques

If an influence diagram contains only discrete probability distributions, one can solve it by converting it into a decision tree and by solving the tree. The most straightforward way to prune a decision tree, known as rollback (see, e.g., Ref. 9), is an application of dynamic programming. It proceeds in reverse chronological order from the endpoints of the tree toward the root node. The expected utility is calculated at each chance node. When a decision node is encountered, the decision alternative with the highest expected utility is selected. As a result, the branch of the tree that leads to the highest expected utility is found. Furthermore, the probability distributions of utility for each decision alternative can be constructed based on the probabilities and the utilities of the solved tree.

A procedure for solving influence diagrams without explicitly converting them into trees is given in Ref. 24. It is also based on dynamic programming, but the terminology is slightly different. The procedure consists of node removals and arc reversals. Except for the utility node, nodes that have arcs into them but not out of them can be eliminated because they do not affect the diagram. A chance node pointing only to the utility node can be reduced by calculating expected utility. A decision node that directly precedes the utility node can be eliminated by choosing the decision alternative with the highest expected utility. If no nodes can be removed directly, arcs between chance nodes are reversed with Bayes' theorem until nodes can be removed again. The diagram will be solved completely by repeating reversals and removals.

If an influence diagram includes continuous probability distributions, it can be solved approximately by Monte Carlo simulation. Another approach would be to discretize the continuous distributions and to solve the resulting decision tree. In Monte Carlo simulation, values of uncertain quantities are generated each according to their own probability distribution. Once all the values have been determined, the expected utility of each decision alternative is calculated. This procedure is repeated sufficiently many times, and the results are recorded. At the end, it is possible to calculate the approximate distributions of expected utility and to examine descriptive statistics of distribution such as the mean, the standard deviation, and the maximum or the minimum of the expected utility.

The presented solution approaches are rather straightforward but laborious to implement. Fortunately, decision support software for structuring and solving influence diagrams are available. For example, PrecisionTree software,[25] which is an add-in for Microsoft Excel, provides all the necessary tools for setting up and analyzing decision trees and influence diagrams. Furthermore, PrecisionTree can be run together with @RISK software,[26] which allows continuous distributions in chance nodes and performs Monte Carlo simulation.

C. Example

We consider an extremely simplified decision problem, in which a missile is pursuing an aircraft. The pilot of the aircraft can implement two defensive maneuvers for avoiding the missile. *Maneuver 1* is aimed at evading a missile approaching from behind, whereas *Maneuver 2* is suitable against missiles approaching from the side. The decision problem of the pilot is to choose the best maneuver. At the decision instant, the pilot does not know the exact geometry, but fortunately he or she can receive an observation on the missile's position before the decision must be made.

The influence diagram representing the decision problem is shown in Fig. 1. The decision alternatives of the *Maneuvering* node are *Maneuver 1* (d_1) and *Maneuver 2* (d_2). The actual missile's position is presented by the chance node *Missile*, and its outcomes, with obvious meanings, are *Tail* (x_1) and *Side* (x_2). We assume that the pilot has enough evidence to assign the probabilities $P(x_1) = 0.4$ and $P(x_2) = 0.6$.

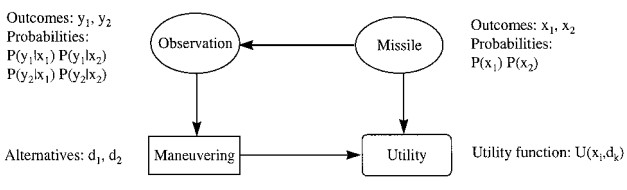

Fig. 1 Example of an influence diagram.

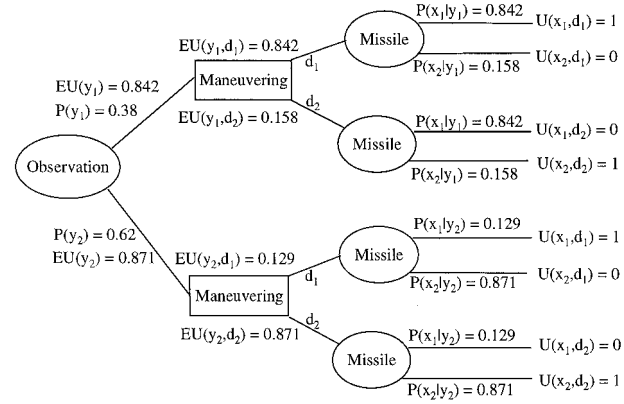

Fig. 2 Decision tree representation of the example influence diagram. EU, expected utility.

The *Observation* node has outcomes *Tail perception* (y_1) and *Side perception* (y_2). If the missile is actually approaching from behind, we hope that the observation is more likely to indicate a tail position rather than a side position and vice versa. Nevertheless, the observation may be incorrect because of, e.g., measurement noise. Thus the *Missile* and the *Observation* nodes are probabilistically dependent and the probabilities of the outcomes y_1 and y_2 are conditional. A possible probability distribution could be $P(y_1 \mid x_1) = 0.8$, $P(y_2 \mid x_1) = 0.2$, $P(y_1 \mid x_2) = 0.1$, and $P(y_2 \mid x_2) = 0.9$.

The pilot prefers *Maneuver 1* in the tail case and *Maneuver 2* in the side case, and thus he or she assesses the following utilities: $U(x_1, d_1) = 1$, $U(x_1, d_2) = 0$, $U(x_2, d_1) = 0$, and $U(x_2, d_2) = 1$.

To demonstrate the connection to decision trees, we transform the example diagram and solve the resulting tree. For this purpose, the arc between the *Missile* and the *Observation* nodes is reversed. Using Bayes' theorem, we can resolve the conditional probabilities $P(x_i \mid y_j)$. The decision tree representation is shown in Fig. 2.

The example decision tree is solved with the rollback procedure. First, the expected utility of each *Missile* node is calculated:

$$\mathrm{EU}(y_j, d_k) = \sum_{i=1}^{2} P(x_i \mid y_j) U(x_i \mid d_k), \qquad j, k = 1, 2 \quad (3)$$

Then, the highest expected utility of the decision nodes is chosen:

$$\mathrm{EU}(y_j) = \max[\mathrm{EU}(y_j, d_1), \mathrm{EU}(y_j, d_2)], \qquad j = 1, 2 \quad (4)$$

The expected utilities are also shown in Fig. 2. The results imply that if *Side perception* is observed, the best maneuvering alternative is *Maneuver 2*. Accordingly, *Tail perception* leads to *Maneuver 1*.

IV. Pilot Decision Model

A. Combat Simulation Model

The pilot decision model aims at producing maneuvering and missile launching decisions for the simulated decision maker in one-on-one air combat. The aircraft of the simulated decision maker is described by a 3-degree-of-freedom point mass model. The evolution of the system state $\boldsymbol{X}$ is represented by the equations of motion:

$$\dot{\boldsymbol{X}} = f(\boldsymbol{X}, n, \mu, u) \quad (5)$$

The state vector $\boldsymbol{X} = [x, y, h, v, \gamma, \chi, m]$ includes variables that refer to the x range, the y range, altitude, velocity, flight path angle, heading angle, and mass. The normal acceleration of the aircraft is controlled with the load factor n and the tangential acceleration with the throttle setting u. The load factor can be directed with the bank angle μ. Gravity and the aircraft mass are assumed constant. Drag coefficients and maximum thrust force of the model refer to a

generic modern fighter aircraft, and the properties of the atmosphere are taken from the international standard atmosphere model.

Values of the control variables are restricted by the constraints

$$n \in [n_{\min}, n_{\max}], \qquad u \in [0, 1], \qquad \mu \in [-\pi, \pi] \tag{6}$$

The feasible region of stationary flight is determined by the minimum altitude and minimum velocity as well as the maximum dynamic pressure constraints. For details of the model, see Ref. 2.

In the influence diagram model the continuous control variables n, u, and μ are replaced with seven discrete control alternatives. Decisions are made at discrete time instants, and the selected control is maintained during a fixed time interval Δt that is called the planning horizon. The control alternatives are the following:

1) Maximal increase of the load factor:

$$n_{\text{com}} = n_{\text{old}} + n_{\Delta}\Delta t, \qquad u_{\text{com}} = u_{\text{old}}, \qquad \mu_{\text{com}} = \mu_{\text{old}}$$

2) Maximal decrease of the load factor:

$$n_{\text{com}} = n_{\text{old}} - n_{\Delta}\Delta t, \qquad u_{\text{com}} = u_{\text{old}}, \qquad \mu_{\text{com}} = \mu_{\text{old}}$$

3) Maximal increase of the bank angle:

$$n_{\text{com}} = n_{\text{old}}, \qquad u_{\text{com}} = u_{\text{old}}, \qquad \mu_{\text{com}} = \mu_{\text{old}} + \mu_{\Delta}\Delta t$$

4) Maximal decrease of the bank angle:

$$n_{\text{com}} = n_{\text{old}}, \qquad u_{\text{com}} = u_{\text{old}}, \qquad \mu_{\text{com}} = \mu_{\text{old}} - \mu_{\Delta}\Delta t$$

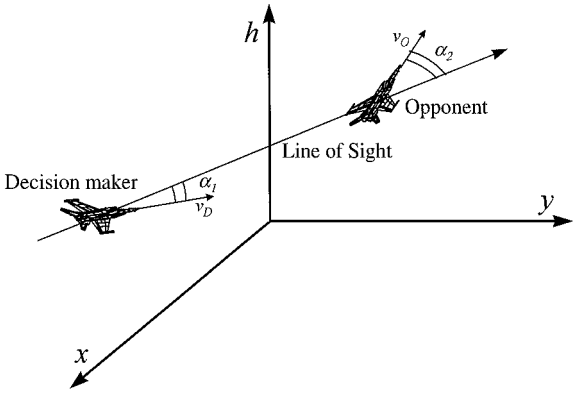

Fig. 3 Relative geometry of air combat.

5) Maximal increase of the throttle setting:

$$n_{\text{com}} = n_{\text{old}}, \qquad u_{\text{com}} = u_{\text{old}} + u_{\Delta}\Delta t, \qquad \mu_{\text{com}} = \mu_{\text{old}}$$

6) Maximal decrease of the throttle setting:

$$n_{\text{com}} = n_{\text{old}}, \qquad u_{\text{com}} = u_{\text{old}} - u_{\Delta}\Delta t, \qquad \mu_{\text{com}} = \mu_{\text{old}}$$

7) The controls are held unchanged:

$$n_{\text{com}} = n_{\text{old}}, \qquad u_{\text{com}} = u_{\text{old}}, \qquad \mu_{\text{com}} = \mu_{\text{old}}$$

Here the subscript com refers to the commanded values of the controls at the decision instant and the subscript old refers to the old values of the controls that were used during the previous planning horizon. The control rates n_{Δ}, μ_{Δ}, and u_{Δ} are fixed. In fact, this scheme introduces an additional order in the dynamics that approximates the pilot and the actuators. The simulated decision maker's predicted states after each control alternative are obtained by integration of the equations of motion with the control alternatives. A maneuver is ignored if it violates the state or the control constraints.

In the model, the relative geometry of the combat situation is described by four attributes: deviation angle α_1, angle off α_2, distance between the players d, and the angle between the players' velocity vectors β (see Fig. 3). Once the positions and the velocity vectors of the players are known in the (x, y, h) frame, the values of the attributes can be calculated.

B. Influence Diagram

The influence diagram representing pilot decision making is shown in Fig. 4. Its overall goals are to suggest whether to launch or not to launch the weapon and to produce combat maneuvers such that the simulated decision maker aims at achieving a firing position and at the same time avoiding the opponent's weapons.

The control decision is modeled by the *Maneuver* node and the use of the weapon by the *Launch Missile* node. The previous node has the control alternatives described in Sec. IV.A. The latter node has two decision alternatives: *Launch the missile* and *Do not launch the missile*.

The values of the predicted states related to each control alternative are given in the deterministic node labeled *Predicted State*. The deterministic node, *Opponent's Predicted State*, contains the exact value of the opponent's state that is described by x range, y range, altitude, flight path angle, heading angle, and velocity. The states of the opponent and the simulated decision maker define the momentary relative geometry that is computed in the *True Geometry* node.

The chance nodes *Sensor 1*, *Sensor 2*, and *Sensor 3*, model the simulated decision maker's observations from the state of the opponent. Here we assume that the pilot can perceive the opponent's state

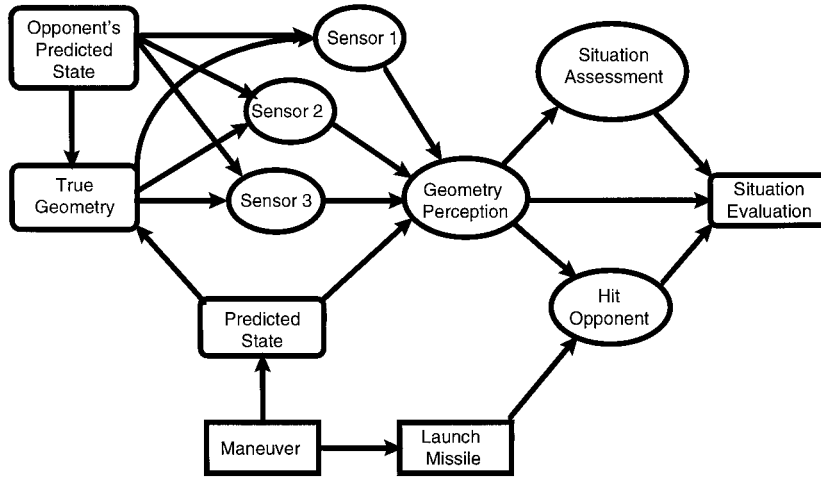

Fig. 4 Influence diagram.

by seeing him or her visually, receiving radio communications from a battle manager, or by detecting him or her with a radar. Each sensor provides a measurement on the opponent's state variables with a given accuracy. The prior probability distributions of the variables are

$$P(x_i) = \frac{1}{\sqrt{2\pi}\sigma_{\mathrm{pr},i}} \exp\left[-\frac{1}{2\sigma^2_{\mathrm{pr},i}}(x_i - \mu_{\mathrm{pr},i})^2\right] \tag{7}$$

where the expected value $\mu_{\mathrm{pr},i}$ and the variance $\sigma^2_{\mathrm{pr},i}$ are fixed by the decision maker's prior belief on the state of the opponent. For sensor j, the observations $y_{i,j} = \{y^1_{i,j}, \ldots, y^{n_j}_{i,j}\}$ on the state variable x_i are assumed to follow a normal distribution whose expected value $\mu_{o,i,j}$ and variance $\sigma^2_{o,i,j}$ depend on the values of the *Opponent's Predicted State* and *True Geometry* nodes. The sensors are assumed unbiased, and thus the expected values are equal to the opponent's exact state and the variance describes the accuracy of the sensor. The posterior distributions are formed by Bayesian reasoning. If the number of observations n_j and the variance $\sigma^2_{o,i,j}$ are known, it can be shown (e.g., Ref. 9) that the posterior distribution $P(x_i \mid y_{i,1}, y_{i,2}, y_{i,3})$ is also a normal distribution whose expected value $\mu_{\mathrm{po},i}$ and variance $\sigma^2_{\mathrm{po},i}$ satisfy

$$\mu_{\mathrm{po},i} = \left(\frac{1}{\sigma^2_{\mathrm{pr},i}}\mu_{\mathrm{pr},i} + \sum_{j=1}^{3}\frac{n_j}{\sigma^2_{o,i,j}}\bar{y}_{i,j}\right) \Bigg/ \left(\frac{1}{\sigma^2_{\mathrm{pr},i}} + \sum_{j=1}^{3}\frac{n_j}{\sigma^2_{o,i,j}}\right) \tag{8}$$

$$\frac{1}{\sigma^2_{\mathrm{po},i}} = \frac{1}{\sigma^2_{\mathrm{pr},i}} + \sum_{j=1}^{3}\frac{n_j}{\sigma^2_{o,i,j}}$$

respectively. Here $\bar{y}_{i,j}$ is the mean of the observations $y_{i,j}$. After the posterior distributions are formed, values of the state variables that are utilized in the *Geometry Perception* node are generated from the posterior distributions.

The chance node *Geometry Perception* represents the simulated decision maker's comprehension of the relative geometry of the current air combat situation. The node includes the same attributes as the *True Geometry* node but, because of the sensors, the combat description attributes are uncertain.

The chance node *Situation Assessment* infers the threat situation of the current air combat from the simulated decision maker's point of view. This node has the following four outcomes:

θ_1 = neutral
θ_2 = advantage
θ_3 = disadvantage
θ_4 = mutual disadvantage

The relative geometry of combat that is associated with each outcome of the *Situation Assessment* node is sketched in Fig. 5. The simulated decision maker's prior beliefs on the situation are given by $P(\theta_1)$, $P(\theta_2)$, $P(\theta_3)$, and $P(\theta_4)$ such that

$$\sum_{i=1}^{4} P(\theta_i) = 1$$

This distribution characterizes the nature of the air combat at a particular time. After the simulated decision maker has observed the values of α_1, α_2, and d, his or her posterior belief on the current air combat situation is, according to Bayesian inference,

$$P(\theta_i \mid \alpha_1, \alpha_2, d) = \frac{P(\theta_i)P(\alpha_1, \alpha_2, d \mid \theta_i)}{P(\alpha_1, \alpha_2, d)}, \qquad i = 1, \ldots, 4 \tag{9}$$

Here α_1, α_2, and d are assumed to be independent random variables and thus

$$P(\alpha_1, \alpha_2, d \mid \theta_i) = P(\alpha_1 \mid \theta_i)P(\alpha_2 \mid \theta_i)P(d \mid \theta_i) \tag{10}$$

The likelihood probability distributions $P(\alpha_1 \mid \theta_i)$, $P(\alpha_2 \mid \theta_i)$, and $P(d \mid \theta_i)$ can be formed by a pilot's experience in air combat. The probability $P(\alpha_1, \alpha_2, d)$ is

$$P(\alpha_1, \alpha_2, d) = \sum_{i=1}^{4} P(\alpha_1, \alpha_2, d \mid \theta_i)P(\theta_i) \tag{11}$$

The probability that a launched missile will hit the opponent is modeled by the chance node labeled *Hit Opponent.* The outcomes are

ϕ_1 = the missile hits
ϕ_2 = the missile does not hit

Prior probability distributions of the uncertain outcomes $P(\phi_1)$ and $P(\phi_2)$ must again be specified in advance. Posterior distributions are calculated with Bayesian reasoning, and they are based on the outcomes of the *Geometry Perception* node.

The preferable actions of the decision maker depend on the current air combat threat situation. Thus each outcome of the *Situation Assessment* node θ_i, $i = 1, \ldots, 4$, and the *Hit Opponent* node ϕ_j, $j = 1, 2$, leads to a different preference ordering. Each combination of the outcomes of the nodes is connected to a different utility function in the *Situation evaluation* node. The utility functions related to the outcome *The missile hits* are

$$u_i(\alpha_1, \alpha_2, \beta, d, L, v) = w^i_{\alpha_1}u^i_{\alpha_1}(\alpha_1) + w^i_{\alpha_2}u^i_{\alpha_2}(\alpha_2) + w^i_{\beta}u^i_{\beta}(\beta) + w^i_d u^i_d(d) + w^i_v u^i_v(v) + w^i_L L, \qquad i = 1, \ldots, 4 \tag{12}$$

and the functions related to the outcome *The missile does not hit* are

$$u_i(\alpha_1, \alpha_2, \beta, d, L, v) = w^i_{\alpha_1}u^i_{\alpha_1}(\alpha_1) + w^i_{\alpha_2}u^i_{\alpha_2}(\alpha_2) + w^i_{\beta}u^i_{\beta}(\beta) + w^i_d u^i_d(d) + w^i_v u^i_v(v) + w^i_L(1 - L), \qquad i = 5, \ldots, 8 \tag{13}$$

Here v is the velocity of the simulated decision maker and L is a binary variable whose value is 1 if the missile is launched and 0 if the missile is not launched. The velocity is taken into account, as it is an important factor for describing the quality of combat states. The aggregating utility functions u_i map the current air combat situation onto a utility scale such that the best outcome has a utility of 1000 and the worst has a utility of 0. Single-attribute utility functions $u^i_{\cdot}$ and weights $w^i_{\cdot}$ describe the preferences of the decision maker. Here, the utility functions are selected somewhat freely to pick the essential characters of critical combat situations. For example, the utility functions of the deviation angle related to each outcome of the *Situation Assessment* node are shown in Fig. 6.

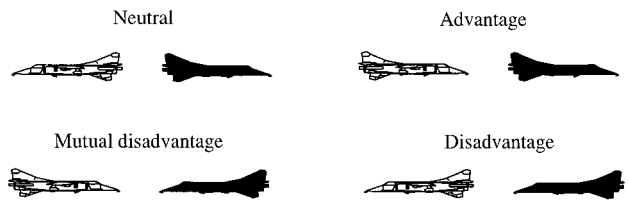

Fig. 5 Sketch of the relative geometry of combat associated with each outcome of the *Situation Assessment* node. Unshaded aircraft, decision maker; shaded aircraft, opponent.

V. Use of the Model

A. Analyzing an Air Combat Situation

We first analyze a single decision in an example air combat situation. At the decision instant, the state of the simulated decision maker is

$$x = 0\,\mathrm{m}, \quad y = 4200\,\mathrm{m}, \quad h = 8000\,\mathrm{m}, \quad v = 300\,\mathrm{m/s}$$

$$\gamma = 0.2\,\mathrm{rad}, \quad \chi = 0\,\mathrm{rad}, \quad m = 10{,}000\,\mathrm{kg}$$

The current values of the control variables are $\mu = 0.5$ rad, $n = 1.5$, and $u = 0.5$, and the control rates are $\mu_\Delta = 1$ rad/s, $n_\Delta = 1$ 1/s, and

$u_\Delta = 0.5$ l/s. The simulated decision maker's states related to each control alternative are predicted with a planning horizon of 1 s.

The exact state of the opponent is $x = 7000$ m, $y = 7000$ m, $h = 10{,}000$ m, $v = 300$ m/s, $\gamma = 0$ rad, and $\chi = 3.14$ rad; i.e., the opponent is approaching the simulated decision maker at a higher altitude from the left.

Let us assume that the simulated decision maker's posterior belief on the opponent's state is the same as the exact state at the decision instant. Therefore the expected values of the posterior distributions of Eq. (7) are equal to the exact values given above and the variances are very small. The prior distributions of the *Situation Assessment* and the *Hit Opponent* nodes are assumed to be as follows:

$$P(\theta_1) = 0.225, \quad P(\theta_2) = 0.175, \quad P(\theta_3) = 0.275$$

$$P(\theta_4) = 0.325, \quad P(\phi_1) = 0.4, \quad P(\phi_2) = 0.6$$

The influence diagram is solved with the PrecisionTree software.[25] In this example, the maximum expected utility (602 utility points) is obtained with the maneuvering alternative, *maximal increase of throttle setting*, with the subsequent decision, *launch the missile*.

Although the decision alternative with the highest expected utility is selected, there is a probability that the coming combat situation will be worse or better than the simulated decision maker assumes. Probability distributions of utility graphically display uncertainty of decisions. The selected decision alternatives lead to the distribution shown in Fig. 7.

Probability distributions of utility can also be constructed for other decision alternatives. The cumulative distributions for each maneuver alternative are shown in Fig. 8. In this picture, dominated and dominating decision alternatives can be identified. For example, the distribution related to the alternative *maximal increase of the throttle setting* lies to the right of the distribution of *maximal increase of the load factor*. Thus one can conclude that the former alternative leads to a better outcome with a higher probability than the latter alternative.

The expected utility is not the only possible measure of a probability distribution. The variance of the distribution measures how widely the values are dispersed in a distribution and thus it is an indication of risk. Minimal and maximal possible utilities indicate the worst and the best possible outcomes that can occur. These quantities for each maneuver alternative in the example combat situation are shown in Table 1.

Table 1 Measures that characterize the probability distributions of utility

	Maneuver						
Statistics	Maximum load	Minimum load	Maximum bank	Minimum bank	Old controls	Maximum throttle	Minimum throttle
Expected	558	537	574	489	590	602	578
Minimum	341	373	362	366	357	367	347
Maximum	673	620	674	584	686	697	674
Variance	105	85	98	85	101	101	101

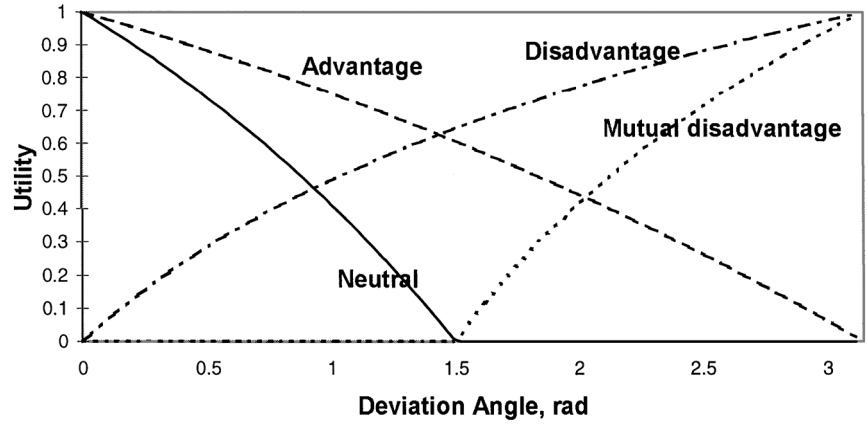

Fig. 6 Utility functions of the deviation angle related to the outcomes of the *Situation Assessment* node. For example, if the threat situation is considered advantageous, the largest utility would be obtained with $\alpha_1 = 0$. On the other hand, if the threat is assessed to be disadvantageous, $\alpha_1 = 0$ is the worst case.

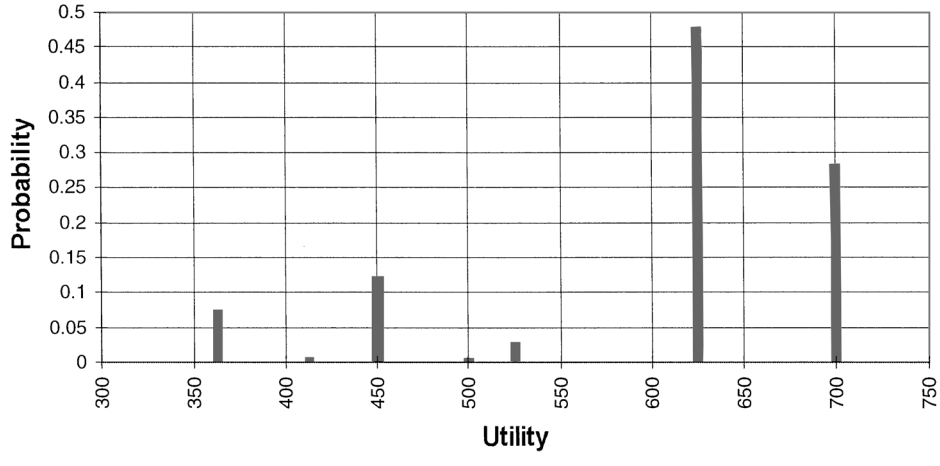

Fig. 7 Probability distribution of utility for the decisions that maximize the expected utility.

In addition to the expected utility, the decision alternative can also be selected on the basis of maximin or maximax criteria.[8] Maximin is the most pessimistic criterion. First, for each alternative the worst possible (minimal) value of utility is identified. Then the alternative whose worst possible utility is highest is chosen. An extremely optimistic decision maker looks at the best that can happen and then the maximax criterion is used. The objective is to find a decision alternative that gives the largest possible utility overall.

B. Sensitivity Analysis

Sensitivity analysis describes the effects of variables on decisions and outcomes. Thus the most important factors in the given decision situation can be found out. One-way sensitivity analysis shows the effect of a single variable on the expected utilities.

As an example, the impact of the opponent's altitude on the maneuvering decision is studied. In the following, the previous air combat situation is referred to as the base case, and all the subsequent results are compared with the outcome of this case.

The opponent's altitude is assumed to be between 9000 and 11,500 m. In the sensitivity analysis, 20 equally spaced values across the altitude range are calculated. The expected utilities related to each maneuver alternative are shown in Fig. 9. The figure shows that as long as the opponent's altitude is between 9375 and 11,250 m, the best maneuver decision is the same as that in the base case. When the altitude decreases below 9375 m, the control alternative *maximal increase of the bank angle* becomes the best decision. If the altitude is above 11,250 m, the best action is to increase the load factor.

One-way sensitivity analysis can also be used to compare the effect of several state variables. Next, we let the y range and the x range vary from 6000 to 8000 m and the altitude from 9000 to 11,000 m, respectively. The results of this analysis are shown in Fig. 10.

The bars of Fig. 10 represent the percentual change of the expected utility when the specified opponent's state variable is varied from one end to the other, keeping all other state variables at their base values. Now the change in the y range seems to have the largest effect on the expected utility, whereas the impact of altitude variation appears to be small. In this way, less important factors of the decision situation can be identified and singled out.

The impact of two variables varying simultaneously can be studied with two-way sensitivity analysis. Typically, the two most critical variables are studied. As an example, two-way sensitivity analysis with respect to the opponent's x and y ranges that vary between 5000 and 9000 m is run. The result is shown in Fig. 11.

Sensitivity analysis can also be utilized in other tasks. A previous study[27] has shown that predetermined combat maneuvers are sensitive to model parameters. The influence diagram can be used

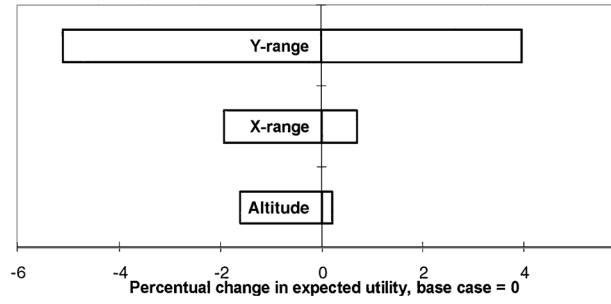

Fig. 10 Impact of the opponent's y range, x range, and altitude variation on the expected utility.

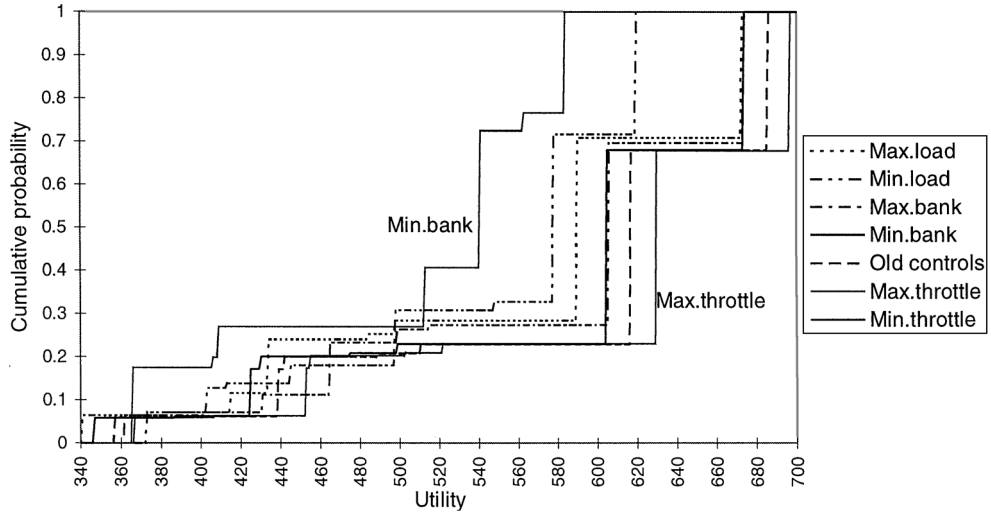

Fig. 8 Cumulative probability distributions of utility for the maneuver alternatives.

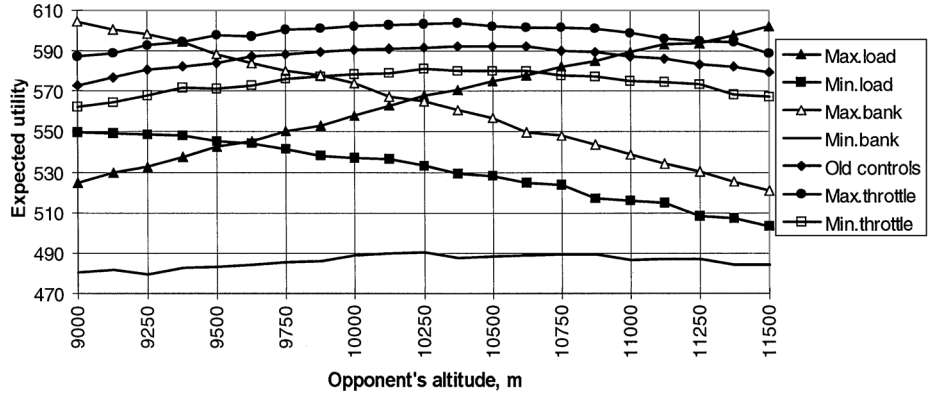

Fig. 9 Sensitivity analysis with respect to the opponent's altitude.

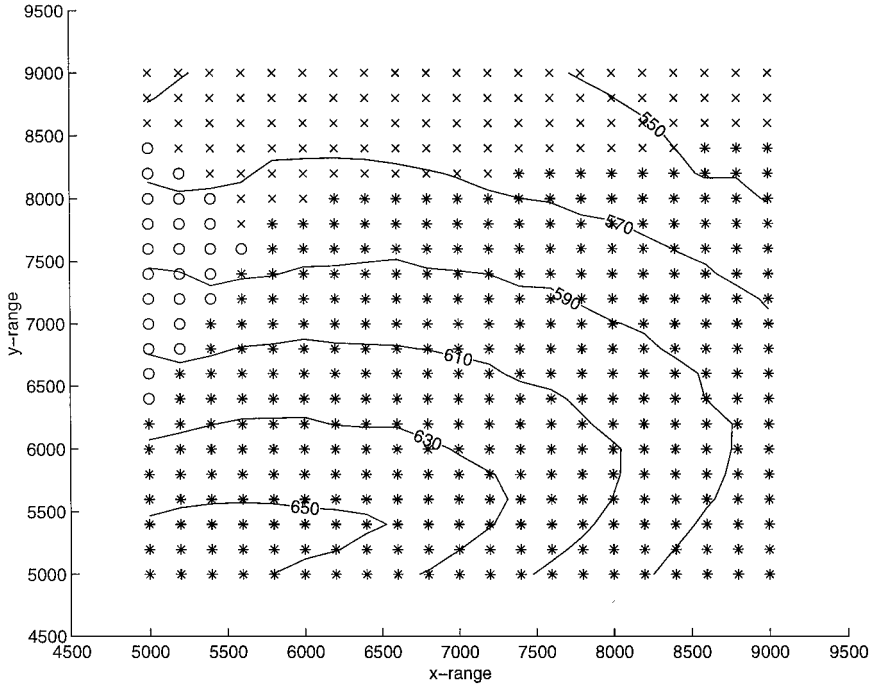

Fig. 11 Regions of the opponent's x and y ranges where different decision alternatives lead to the highest expected utility together with the contours of the expected utility in 20 utility point intervals. ∗, maximal increase of the throttle setting; ×, maximal increase of the bank angle; and ∘, maximal increase of the load factor.

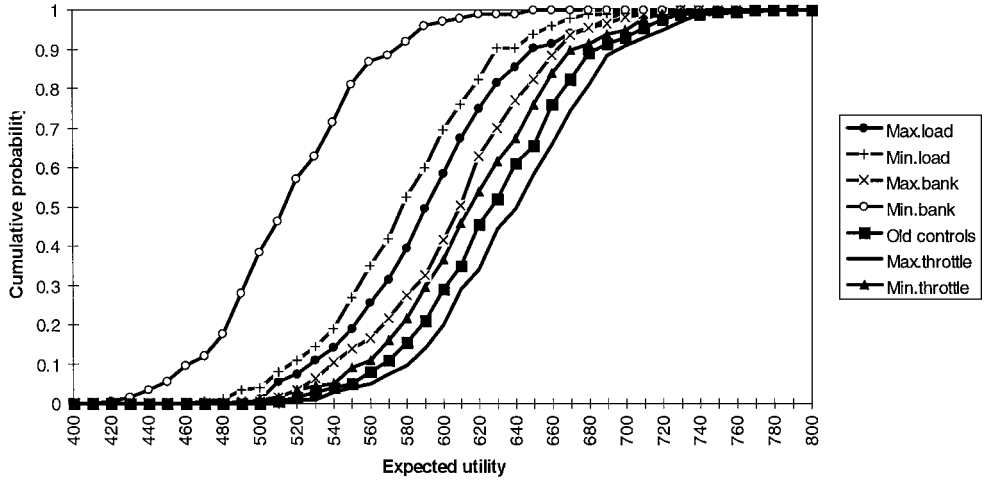

Fig. 12 Cumulative probability distributions of expected utility when the decision is made based on a priori information.

to extend this analysis to assess the impact of parameters on the pilot's decisions and the outcome of a combat. Among other things, effects of maximum thrust force or drag coefficients can be studied. On the other hand, the influence of the pilot's preferences, resulting from tactics, training, and doctrine, can be analyzed by varying the weights and by changing the shape of the utility functions.

C. Effect and Value of Sensor Information

The nodes *Sensor 1*, *Sensor 2*, and *Sensor 3* model the simulated decision maker's information gathering. Since they contain continuous probability distributions, the impact of new information can be studied by Monte Carlo simulation. In this example, maneuver alternatives are ordered according to the mean of the expected utility. The difference between means of expected utility is used as a measure of the value of information.

In practice, the simulated decision maker does not know the opponent's exact state. Let us assume that his or her prior belief on the opponent's state is the same as the base case state, but the opponent's true state is actually $x = 5000$ m, $y = 5000$ m, $h = 8000$ m, $v = 300$ m/s, $\gamma = 0$ rad, and $\chi = 1.5$ rad. Expected values of the sensor distributions $\mu_{o,i,j}$ are equal to the opponent's true state. Accuracy of the sensors is different such that sensor 3 is the most accurate and sensor 1 is the most inaccurate. Consequently the variance of the distribution that models sensor 3 is assumed small and the variance related to the sensor 1 large.

First, the simulated decision maker does not receive extra information, and thus the executed decision alternative is chosen based on his or her prior belief on the opponent's state. The cumulative probability distributions of the expected utility for each maneuver alternative are shown in Fig. 12. The maneuver alternative *maximal increase of the throttle setting* produces the highest mean of expected utility, 644 utility points. Furthermore, this maneuver alternative ensures the highest expected utility in the worst and the best possible cases.

If the simulated decision maker had access to perfect state information, the maneuver alternative *maximal decrease of the load*

Table 2 Preferable maneuver alternatives, maximum means of expected utility, and value of extra information related to different sensor information

Case	Number of observations			Alternative	Mean EU	Value
	Sensor 1	Sensor 2	Sensor 3			
Prior	——	——	——	Maximum throttle	644	——
1	1	0	0	Maximum throttle	679	35
2	1	1	0	Maximum throttle	695	51
3	1	1	1	Maximum bank	715	71
4	10	0	0	Maximum bank	716	72
5	10	10	0	Minimum load	732	88
6	10	10	10	Minimum load	739	95
Perfect	——	——	——	Minimum load	745	101

factor would lead to the highest mean of expected utility, 745. Thus the value of perfect information with the given prior belief is $745 - 644 = 101$.

Next, the influence diagram is solved six times with different combinations of the sensors and numbers of observations. The summary of the results is shown in Table 2. For example, in the fourth case, the simulated decision maker receives 10 observations from sensor 1. The maximum mean of expected utility (716) is obtained with the maneuver alternative *maximal increase of bank angle* and the value of this information is $716 - 644 = 72$.

The value of information approaches the value of perfect information when the simulated decision maker makes more observations. Furthermore, the change of the preferable maneuver alternative is identified. For example, 10 observations with sensors 1 and 2 are required for selecting the correct maneuver alternative.

When the pilot decision model is analyzed with different information, impacts of the sensors on the outcome of the pilot's decision situation can be determined. In this way, effects of sensor accuracy can be studied and the most important, as well as critical, sensors can be specified.

VI. Model Extension

A. Improvements

The presented examples illustrate the utilization of the influence diagram in the analysis of a pilot's decision problems. However, influence diagram methodology offers several possibilities to refine the model. Here we list some potential improvements.

As mentioned above, the utility functions and the probability distributions of the model are assigned rather informally. True preferences and behavior of human pilots can be captured into an influence diagram by composing utilities and probabilities in cooperation with human pilots during the evolution phase of a model. The utility assessment would produce information on interdependencies of the attributes that would possibly require the use of multiplicative utility functions.

The numerical treatment of normal distributions is straightforward, but it is not clear whether they are adequate for describing different sensors. Thus the sensor models could be improved if more realistic distributions are used. In the implementation of the model, other sensors like a radar warning receiver or a forward-looking infrared system should also be modeled.

The missile system is described by an ad hoc probability of hit. A modification to a diagram should include more realistic missile systems that consist of guidance laws and aerodynamic models. Probabilities of hit produced by real weapons systems could also be utilized. Furthermore, models of guns should possibly be considered.

In the presented diagram, the opponent's state is modeled with deterministic variables. To achieve more realism, the opponent's future state can be predicted by making presumptions about the opponent's behavior. In the game models,[15,16] the opponent is assumed to act in the worst possible way. This idea can be taken into account by adding a chance node that represents the maneuvering decision of the opponent. Furthermore, the players' future states should be predicted further than one planning horizon ahead. In practice, a model of this type can be considered as a sequence of influence diagrams.

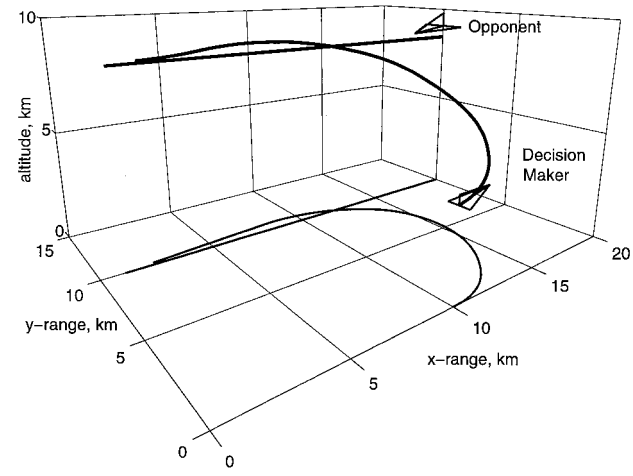

Fig. 13 Example trajectory of the decision maker against a nonmaneuvering opponent. Note that in the beginning the decision maker correctly avoids the front sector of the opponent.

B. Use in Simulation

In addition to the analysis presented above, the influence diagram model could also be used as a guidance system that selects combat maneuvers in air combat simulation. At the beginning of the simulation, the prior probability distributions of the model are assumed to be uniform. During the simulation, the probabilities can be updated such that the prior distributions at the current decision instant are associated with the posterior probabilities of the previous decision instant. A simple example is presented in Fig. 13, in which the trajectory of the simulated decision maker against a nonmaneuvering target is produced with these ideas.

C. Extension to M-on-N Combat

An influence diagram could also be extended into situations in which there are several opponents and friendly aircraft. In an M-on-N air combat simulation, friendly resources must be distributed by assessing opponents from among the group of hostile aircraft for each friendly aircraft. Since the resources are allocated by a battle manager, M-on-N air combat simulation needs a model that emulates his or her behavior. Such a model, also implemented by influence diagrams, has actually been introduced in Ref. 13. The objective of this model is to allocate the optimal number and type of aircraft and munitions against each target in an air mission planning procedure.

After the allocation, each combat can be described by a separate influence diagram. A case with only one friendly aircraft and several opponents can be modeled by extending the influence diagram presented in this paper to contain deterministic nodes that model the states of new opponents. Furthermore, new outcomes representing possible threat situations must be added, and utility functions related to these outcomes must be created. The probability of hit with respect to each enemy aircraft must also be defined.

If several friendly aircraft attend a combat, it is more difficult to expand the model. Now the diagram must contain decision nodes representing decisions for each simulated decision maker. The model must capture the joint objectives and goals of a group. It might be possible to construct a group utility function (see, e.g., Ref. 28) that offers a tool for implementing cooperative tactics for friendly aircraft. On the other hand, a command chain is not difficult to implement. For example, a flight leader can be modeled by modifying the diagram such that the decision node of the flight leader precedes the decision nodes of the wing men. An alternative approach to implement commands is to use different utility functions associated with different missions.

VII. Conclusion

In the complex and transient setting of an air combat, pilots face complicated decision-making problems and thus it is not easy to

choose the actions that lead to the best possible outcomes. A model that imitates pilot decision making must have the capability to evaluate decision alternatives under multiple conflicting objectives whose outcomes are known only under conditions of uncertainty. A pilot decision-making model must also be able to model and utilize new information that may reduce uncertainty. These features are available in the presented influence diagram model.

The examples of this paper show how the decision situations of a pilot can be analyzed. The result of the analysis is the overall probability distributions of utility for each maneuver alternative. The utility score represents the pilot's evaluation of the combat situation. Based on the distributions of the utility, rational and reasonable maneuvering decisions in the light of all the available information are obtained. Sensitivity analysis can be carried out to determine the factors that are the most important and critical in a given decision situation. Furthermore, the value and the effect of new observations on the opponent can be analyzed. In this way, one can evaluate, for example, the possible benefits of new sensors.

Overall, an influence diagram analysis provides a structural and clear way to analyze the pilot's preferences as well as to compare the performance of different aircraft and technologies. This new approach holds a lot of promise for improving the understanding of pilot decision making in air combat.

Acknowledgment

The authors thank the Finnish Air Force for support and collaboration.

References

[1]Raivio, T., Ehtamo, H., and Hämäläinen, R. P., "Aircraft Trajectory Optimization Using Nonlinear Programming," *System Modeling and Optimization*, edited by J. Dolezal and J. Fidler, Chapman and Hall, London, 1996, pp. 435–441.

[2]Virtanen, K., Ehtamo, H., Raivio, T., and Hämäläinen, R. P., "VIATO—Visual Interactive Aircraft Trajectory Optimization," *IEEE Transactions on Systems, Man, and Cybernetics, Part C, Applications and Reviews*, Vol. 29, No. 3, Aug. 1999.

[3]Raivio, T., Ehtamo, H., and Hämäläinen, R. P., "A Decomposition Method for a Class of Pursuit-Evasion Games," *Proceedings of the 7th International Symposium on Differential Games and Applications*, Vol. 2, International Society of Dynamic Games, Helsinki, 1996, pp. 784–795.

[4]Bent, N. E., "The Helicopter Air-to-Air Value Driven Engagement Model (HAVDEM)," *Proceedings of the 19th ICAS Congress*, ICAS-94-8.6.1, International Council of the Aeronautical Sciences, Les Mureaux, France, 1994, pp. 2181–2189.

[5]Goodrich, K. H., and McManus, J. W., "Development of A Tactical Guidance Research and Evaluation System (TiGRES)," AIAA Paper 89-3312, Aug. 1989.

[6]Lazarus, E., "The Application of Value-Driven Decision-Making in Air Combat Simulation," *Proceedings of the IEEE International Conference on Systems, Man, and Cybernetics*, Institute of Electrical and Electronics Engineers, New York, 1997, pp. 2302–2307.

[7]Stehlin, P., Hallkvist, I., and Dahlstrand, H., "Models for Air Combat Simulation," *Proceedings of the 19th ICAS Congress*, ICAS-94-8.6.2, International Council of the Aeronautical Sciences, Les Mureaux, France, 1994, pp. 2190–2196.

[8]Bunn, D., *Applied Decision Analysis*, McGraw-Hill, New York, 1984.

[9]Clemen, R. T., *Making Hard Decisions, An Introduction to Decision Analysis*, 2nd ed., Duxbury Press, Belmont, CA, 1996.

[10]Keeney, R., and Raiffa, H., *Decision with Multiple Objectives*, Wiley, New York, 1976.

[11]Von Winterfeldt, D., and Edwards, W., *Decision Analysis and Behavioral Research*, Cambridge Univ. Press, Cambridge, England, UK, 1986.

[12]Howard, R. A., and Matheson, J. E., "Influence Diagrams," edited by R. A. Howard, and J. E. Matheson, *The Principles and Applications of Decision Analysis*, Vol. 2, Strategic Decision Group, Palo Alto, CA, 1984, pp. 719–762.

[13]Griggs, B. J., Parnell, G. S., and Lehmkuhl, J. L., "An Air Mission Planning Algorithm Using Decision Analysis and Mixed Integer Programming," *Operations Research*, Vol. 45, No. 5, 1997, pp. 662–676.

[14]McManus, J. W., and Goodrich, K. H., "Application of Artificial Intelligence (AI) Programming Techniques to Tactical Guidance for Fighter Aircraft," AIAA Paper 89-3525, Aug. 1989.

[15]Austin, F., Carbone, G., Falco, M., and Hinz, H., "Game Theory for Automated Maneuvering During Air-to-Air Combat," *Journal of Guidance, Control, and Dynamics*, Vol. 13, No. 6, 1990, pp. 1143–1149.

[16]Katz, A., "Tree Lookahead in Air Combat," *Journal of Aircraft*, Vol. 31, No. 4, 1994, pp. 970–973.

[17]Burgin, G. H., and Sidor, L. B., "Rule-Based Air Combat Simulation," NASA CR-4160, 1988.

[18]Basar, T., and Olsder, G., *Dynamic Noncooperative Game Theory*, 2nd ed., Academic, London, 1995, pp. 20–31.

[19]Henrion, M., Breese, J. S., and Hortvitz, E. J., "Decision Analysis and Expert Systems," *Artificial Intelligence Magazine*, Vol. 12, No. 4, 1991, pp. 64–91.

[20]Oliver, R. M., and Smith, J. Q., *Influence Diagrams, Belief Nets and Decision Analysis*, Wiley, New York, 1989, Chaps. 1–4.

[21]Hämäläinen R. P., and Lauri, H., "HIPRE 3+ User's Guide," Systems Analysis Laboratory, Helsinki University of Technology, Finland, 1992, URL: http://www.hipre.hut.fi.

[22]Savage, L. J., *The Foundations of Statistics*, Wiley, New York, 1954.

[23]Spetzler, C. S., and Stael von Holstein, C. A., "Probability Encoding in Decision Analysis," *Management Science*, Vol. 22, No. 3, 1975, pp. 340–352.

[24]Shachter, R. D., "Evaluating Influence Diagrams," *Operations Research*, Vol. 44, No. 6, 1986, pp. 871–882.

[25]PrecisionTree, User's Guide, Palisade Corp., New York, 1996.

[26]@RISK, User's Guide, Palisade Corp., New York, 1996.

[27]Hoffren, J., and Vilenius, J., "Sensitivity of Air Combat Maneuvers to Aircraft Modeling Uncertainties," AIAA Paper 98-4165, Aug. 1998.

[28]Keeney, R., and Kirkwood, C. W., "Group Decision Making Using Cardinal Social Welfare Functions," *Management Science*, Vol. 22, No. 4, 1975, pp. 430–437.